Дмитро Валерійович Портнягін

Моделювання циклічної роботи літієвої батареї з мікропористим вуглецевим електродом

Роботу отримано 1 вересня 2006 р.

Затверджено до друку Вченою радою ІФКС НАН України

Рекомендовано до друку семінаром відділу теорії нерівноважних процесів

Виготовлено при ІФКС НАН України

Національна академія наук України

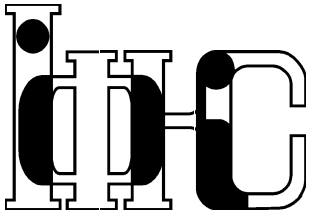

ІНСТИТУТ ФІЗИКИ КОНДЕНСОВАНИХ СИСТЕМ

ICMP–06–10E

Dmitry Portnyagin*

MODELLING OF CYCLING OF LITHIUM BATTERY WITH MICROPOROUS CARBON ELECTRODE

*E-mail: port@icmp.lviv.ua

ЛЬВІВ

УДК: 541.13; 53.072; 53:681.3; 539.219.3; 538.931-405

PACS: 82.47.Aa, 82.45.Gj, 82.45.Fk, 82.45.-h, 82.20.Wt

Моделювання циклічної роботи літієвої батареї з мікропористим вуглецевим електродом

Д.В. Портнягін

Анотація. Моделювалася циклічна зарядка-розрядка літієвої батареї із вуглецевим мікропористим електродом в режимі заданої напруги. Порівнювалися передбачення двох моделей: без електростатичного поля та з електростатичною взаємодією всередині частинок вуглецевого електрода. Спостерігалася певна розбіжність між ними.

Modelling of cycling of lithium battery with microporous carbon electrode

D.V. Portnyagin

Abstract. Cycling of lithium cell with microporous carbon electrode under potentiodynamic control has been modelled. Predictions of the models without electric field and with electrostatic interaction inside the particles of carbon electrode have been compared. It has been observed a considerable difference between both.

Подається в Condensed Matter Physics
Submitted to Condensed Matter Physics

1. Introduction.

Rapid development in recent years in the market of mobile phones, laptop computers, other portable devices and electric vehicles evoke the demand for a high energy density portable power sources. In such batteries lithium often serves as a cathode material because of its low electronegativity. Porous materials are used for anode due to their large surface area associated with high energy storage. Mathematical simulation of charge/discarge processes allows to optimize the battery in order to obtain a higher performance. This can also help to analyze these processes to gain a deeper insight into the nature and courses of phenomena that occur during the cycling of these devices. Recently the simulation of the intercalation of lithium into the structure of porous electrode has been attracting the attention of several authors [3], [1], [5]. It is widely held that the main driving force at the operation of the battery is diffusion and that the transport of ions across the electrode is governed by Fick's second law. In the present paper we have made an improvement on this approach by taking into account electrostatic interaction between ions and with the distribution of charge in the bulk of porous electrode. Comparison of the predictions of the diffusive and the more realistic electrodynamic model testifies to that there is a certain discrepancy between them.

2. Basic considerations. Cylindrical particles.

We study the cycling of lithium battery under potentiodynamic control. In our research we heavily rely upon the data from [1]. The battery consists of lithium foil, porous separator of thickness $L_s = 25\mu m$, porous carbon electrode of thickness $L_1 = 125\mu m$ made of either cylindrical or spherical particles of radius $R_s = 3,5\mu m$, and current collector. The battery is immersed in 1M solution of $LiClO_4$ in propylene carbonate.

The applied potential is changed linearly with time and is given by

$$U_{app} = U_0 + \omega t$$

where U_0 is the initial applied potential, ω is the sweep rate, t is time. At a sweep rates 10, 5 and 1 mV/s the battery was discharged from its initial state to 0.075V, then it was charged to 1.5 V, after that the battery was again discharged to 0.075V. These steps were repeated twice to reach a periodic state. The periodic state is the state, at which the results are uniform and sustained during consecutive cycles, when cycled under the same conditions.

During the discharge of the battery, lithium is dissolved into lithium ions from the negative electrode, migrates through the separator and finally intercalates into the carbon electrode. During the charge the reverse process takes place. We neglect the electrodes expansion and contraction. There exist two approaches for modelling lithium insertion into the particle, both of which lead to solving the diffusion equation in a particle. In the first approach the driving force is the gradient of concentration while the diffusion coefficient remains constant. However, it has been reported that there is a strong dependence of the diffusion coefficient on concentration due to the lithium ion-lithium ion interactions inside the particle, which can not be ignored to obtain good agreement with experimental data. In the second approach Verbrugge and Koch [6] considered the gradient of the chemical potential of the inserted lithium ions as the driving force.

In the present section we consider cylindrical particles with the ratio of length to radius sufficiently large, for which the concentration of lithium inside the particle is a function only of radial distance, governed by the equation

$$\frac{\partial y}{\partial \tau} = \frac{1}{R}\frac{\partial}{\partial R}\left(Rf\frac{\partial y}{\partial R}\right) \tag{2.1}$$

$$y = y_0, \quad \text{at} \tau = 0, \forall R; \tag{2.2}$$

$$\frac{\partial y}{\partial R} = 0 \quad \text{at} R = 0, \forall \tau; \tag{2.3}$$

$$\frac{\partial y}{\partial R} = -\frac{j_n^+}{D_s}\frac{R_s}{C_{s,max} f} \quad \text{at} R = 1, \forall \tau; \tag{2.4}$$

where $\tau = tD_s/R_s^2$, $y = C_s/C_{s,max}$, $R = r/R_s$; are dimensionless variables. D_s is the diffusion coefficient in the solid phase, assumed to be constant, R_s is the radius of the particle, C_s is the concentration of lithium ions inside the particle, $C_{s,max}$ is the maximum concentration of lithium ions inside the particle, f is the activity factor dependant on the intercalation fraction and calculated by Verbrugge and Koch [6], j_n^+ is the flux of lithium ions at the surface of the particle. The initial value of y is equal to 0.01. The flux of lithium ions at the surface of the particle is equal to the electrochemical reaction rate per unit of surface area of the particle as given by a Butler-Volmer reaction rate expression

$$j_n^+ = K\left(C(1-y\big|_{R=1})\right)^{\beta-1}\left(y\big|_{R=1}\right)^{\beta} \times \left\{\exp\left[\frac{(1-\beta)F}{\Re T}(\eta - U)\right] - \exp\left[\frac{-\beta F}{\Re T}(\eta - U)\right]\right\},$$

where C is the concentration of the electrolyte, K is the reaction rate constant ($K = k_c^{1-\beta}k_a^{\beta}$), F is the Faraday constant, $\Re$ is universal gas constant, T is temperature, η is the potential between solid phase and electrolyte, and U represents the open-circuit cell potential with respect to a metallic lithium electrode which is evaluated at the surface of the particle where the electrochemical reaction takes place and which is given by

$$U = U_s + \frac{\Re T}{F}\ln\left(\frac{1-y\big|_{R=1}}{y\big|_{R=1}}\right) - \sum_{s=2}^{7}\frac{\Omega_s}{F}s(y\big|_{R=1})^{s-1} \quad \text{for} \quad 0 < y|_{R=1} < 0.985,$$

where U_s is the standard cell potential with respect to a metallic lithium electrode, and Ω_s are the self-interaction energies. We take the activity coefficient

$$f = 1 \tag{2.5}$$

for purely diffusive model, and

$$f = \left(1 + \frac{d\ln\gamma_+}{d\ln y}\right) = 1 + \sum_{s=2}^{7}\frac{\Omega_s}{\Re T}s(s-1)(y^{s-1} - y^s) \tag{2.6}$$

for chemical potential model (at low lithium concentrations f increases with increasing the lithium ion concentration due to repulsive effects, takes on its maximum at $y = 0.2$, and decreases with increasing the lithium ion concentration due to low ion mobility at higher concentrations). Our amendment to the aforementioned models consists in adding the current coursed by electric field to the righthand side of equation (2.1).

$$\frac{\partial y}{\partial t} = \frac{1}{R}\frac{\partial}{\partial R}\left(R\frac{D_s}{R_s^2}f\frac{\partial y}{\partial R}\right) - \frac{1}{FC_{max,s}}\mathrm{div}(\sigma E), \tag{2.7}$$

where E is the electric field, σ the ionic conductivity given by Einstein relation

$$\sigma = yC_{max,s}N_aD_se^2/kT,$$

k is Boltzman constant, e is elementary charge, N_a is Avogadro number.

In the first approximation we assume that the current of positive ions through the surface of the particle is entirely due to the uniform distribution within the particle of negative charge, which carbon, being more electronegative, draws from lithium, and the distribution of charge caused by imposed external electric field. However, X-ray photoelectron

spectroscopy (XPS) proved [4] that after insertion the lithium retains only a fraction of the positive charge $+\delta$, while the carbon takes a negative charge $-\delta$. Therefore to the distribution of charge in the bulk of the particle we add the term associated with the nonuniform distribution of lithium ions. This results in

$$\mathrm{div}(E) = \frac{2}{R_s \sigma_{eff,1}} j_n^+ - \delta \frac{F C_{max,s}}{\varepsilon_0}(y_{avr} - y),$$

where $\sigma_{eff,1}$ is the effective conductivity of electrolyte in the carbon electrode, ε_0 is the dielectric constant, $y_{avr} = \int y dV/V = 2\int\limits_0^1 yRdR$ (or $= 3\int\limits_0^1 yR^2 dR$ for spherical particles) is the average concentration of ions in the particle, δ is the delocalization factor which equals 1 when we have naked lithium ions and negative charge, drawn from lithium, uniformly spread over carbon sites, and equals 0 when negative charge is maximally localized on lithium ions.

We shall refer to the insertion of lithium ions as a process given by the solution of (2.1)-(2.4) with f given by (2.5) the (DFM) model, and with f given by (2.6) - the (CPM) model. We shall call the diffusion process described by (2.7), (2.2)-(2.4) with f given by (2.5) the (DFME) model, and with f given by (2.6) - the (CPME) model.

The ionic current across the carbon electrode i_2 is equal to the external current through the battery i_{total} at the contact with separator, and is zero at current collector. Between these two values the current is assumed to be distributed according to the equaiton:

$$\frac{\partial i}{\partial x} = aF j_n^+,$$

where a is the interfacial area of particles per unit volume of porous electrode, calculated by

$$a = 0.03 \cdot 2(1-\epsilon_1)/Rs,$$

for the case of cylindrical particles, or by

$$a = 0.02 \cdot 3(1-\epsilon_1)/Rs$$

for spherical; ϵ_1 - porosity of carbon electrode. It appears quite obvious that after we have pressed and baked the carbon material, only a fraction of the particle's surface will be exposed to electrolyte, so we have introduced a suitable factor in the formula for the interfacial area. The

equation for the concentration of the electrolyte in the solution phase of the carbon electrode is

$$\epsilon_k \frac{\partial C}{\partial t} = \nabla\left(\epsilon_k D_{eff,k} \nabla C\right) + a(1-t_+^0) j_n^+,$$

where $k = 1, s$ (1 corresponds to electrode, s to separator), t_+^0 is transfer number, $D_{eff,k} = \epsilon_k^{0.5} D$, D is the diffusion coefficient of electrolyte, $C_{initial} = 1000 \quad mol/m^3$. We impose on C the following boundary conditions: (i) that the flux of ions at lithium electrode is equal to the total current through the cell

$$\epsilon_s D_{eff,s} \nabla C\big|_{x=L_s+L_1} = i_{total}/F,$$

(ii) that the flux of mass is continuous at the separator-electrode interface

$$\epsilon_s D_{eff,s} \nabla C\big|_{x=L_s+0} = \epsilon_1 D_{eff,1} \nabla C\big|_{x=L_s-0},$$

and (iii) that its's equal to zero at current collector

$$\epsilon_1 D_{eff,1} \nabla C\big|_{x=0} = 0.$$

The potential in the solution phase is

$$\nabla \phi_1 = -\frac{i_2}{\sigma_{eff,k}} + \frac{\Re T(1-t_+^0)}{FC} \nabla C,$$

where $\sigma_{eff,k}$ is the effective conductivity of electrolyte given in Table I. The potential in the solid phase of the electrode is

$$\nabla \phi_2 = -\frac{(i_{total} - i_2)}{\sigma_{eff}},$$

where $\sigma_{eff} = \epsilon_1^{1.5} \sigma_{el}$ is the effective conductivity of electrode. The local surface overpotential is given by

$$\eta = \phi_1 - \phi_2.$$

The applied potential of the cell is related to η by

$$U_{app} = \eta\big|_{x=L_s+L_1} + (\phi_1 - \phi_2)_{kin} + \int\limits_{x=0}^{x=L_1} \frac{[i_{total} - i_2(x)]}{\sigma_{eff}},$$

where $(\phi_1 - \phi_2)_{kin}$ is given by kinetic expression

$$i_{total} = FK_{Li}C^{0.5}(\exp((0.5F/(\Re T))(\phi_1 - \phi_2)) - \\ - \exp(-(0.5F/(\Re T))(\phi_1 - \phi_2)))$$

with K_{Li} - the reaction rate constant at the lithium electrode.

All the parameters of the cell are evaluated at $T = 298K$ for the reasons explained in [2]. The values of the standard cell potential, the self-interaction energies, and the kinetic parameters are given in Table I.

The corresponding set of equations from Table II has been solved numerically.

Let us clear up how the speed of changing of j_n^+ during the cycling depends on the speed of changing of applied voltage U_{app}. We have, approximately,

$$\frac{d}{dt}j_n^+ = KC^{\beta-1}\left[(\beta-1)\left(1-y\big|_{R=1}\right) - \beta\left(y\big|_{R=1}\right)\right] \times \\ \left(1-y\big|_{R=1}\right)^{\beta-2}\left(y\big|_{R=1}\right)^{\beta-1} \times \\ \left\{\exp\left[\frac{(1-\beta)F}{\Re T}(U_{app}-U)\right] - \exp\left[\frac{-\beta F}{\Re T}(U_{app}-U)\right]\right\}\frac{dy}{dt} + \\ + KC^{\beta-1}\frac{F}{\Re T}\left(1-y\big|_{R=1}\right)^{\beta-1}\left(y\big|_{R=1}\right)^{\beta} \times \\ \left\{(1-\beta)\exp\left[\frac{(1-\beta)F}{\Re T}(U_{app}-U)\right] + \right. \\ \left. + \beta\exp\left[\frac{-\beta F}{\Re T}(U_{app}-U)\right]\right\}\left[\frac{U_{app}}{dt} - U'\frac{dy}{dt}\right].$$

Substituting for $\frac{dy}{dt}$ its expression from the diffusion equation in which we neglect electrostatic interaction, and substituting 1 for y and its spacial derivatives, since they are dimensionless magnitudes, hence we get the following estimate for the order of magnitude:

$$\frac{d}{dt}j_n^+ \simeq j_n^+\left(1+\sum_{s=2}^{7}\frac{\Omega_s}{\Re T}\right)\frac{D_s}{R_s^2} + \\ + (\pm 1)j_n^+\left\{\frac{\beta F}{\Re T}\frac{U_{app}}{dt} - \beta\left(1+\sum_{s=2}^{7}\frac{\Omega_s}{\Re T}\right)^2\frac{D_s}{R_s^2}\right\}, \quad (2.8)$$

Table I. Standard cell potential, interaction energies, model parameters for the carbon-lithium cell and physical constants.

Parameter	Value
U_0	$0.91489 \quad V$
U_s	$0.8170 \quad V$
Ω_2/F	$0.9926 \quad V$
Ω_3/F	$0.8981 \quad V$
Ω_4/F	$-5.630 \quad V$
Ω_5/F	$8.585 \quad V$
Ω_6/F	$-5.784 \quad V$
Ω_7/F	$1.468 \quad V$
$C_{s,max}$	$18,000 \quad mol/m^3$
β	0.5
K	$3.28 \times 10^{-6} \quad mol^{1/2}/m^{1/2}s$
K_{Li}	$4.1 \times 10^{-6} \quad mol^{1/2}/m^{1/2}s$
$C_{initial}$	$1000 \quad mol/m^3$
T	$298 \quad K$
$y_{initial}$	0.01
D	$2.6 \times 10^{-10} \quad m^2/s$
D_s	$1.0 \times 10^{-14} \quad m^2/s$
t_+^0	0.2
$\sigma_{eff,k}$	$\epsilon_k^{1.5}C^{0.855}(0.00179\exp(-0.08(0.00083C-0.6616)^2 - 0.0010733C+0.855)) + 0.0001$
σ_{el}	$100 \quad S/m$
R_s	$3.5 \times 10^{-6} \quad m$
L_s	$25 \times 10^{-6} \quad m$
L_1	$125 \times 10^{-6} \quad m$
k	$1.381 \times 10^{-23} \quad J/K$
N_a	$6.022 \times 10^{23} \quad mol^{-1}$
$\Re$	$8.314 \quad J/(mol \cdot K)$
F	$96,487 \quad C/mol$
ε_0	$8.854 \times 10^{-12} \quad C^2/(N \cdot m^2)$
e	$1.9 \times 10^{-19} \quad C$
δ	2×10^{-10}
ϵ_1	0.35
ϵ_s	0.55

where we take "+" when j_n^+ is positive, "-" when it is negative. Hence

we can conclude that the hysteresis is the more significant, the steeper is the relation graph of j_n^+ vs. applied voltage, and the stronger, in turn, is the following inequality:

$$\frac{U_{app}}{dt} \gg \frac{\Re T}{F}\left(1+\sum_{s=2}^{7}\frac{\Omega_s}{\Re T}\right)^2\frac{D_s}{R_s^2}. \qquad (2.9)$$

And vice versa, the hysteresis is the less significant, the stronger is the reverse inequality:

$$\frac{U_{app}}{dt} \ll \frac{\Re T}{F}\left(1+\sum_{s=2}^{7}\frac{\Omega_s}{\Re T}\right)^2\frac{D_s}{R_s^2} \qquad (2.10)$$

(in this case $\frac{d}{dt}j_n^+$ dose not become large, because the whole righthand side in (2.8) is multiplied by the derivative of y with respect to radial distance, which, the concentration profile being sloping, is small). The above said is verified by Figures 9 and 10.

One can see from Figure 1 that in the case of a constant diffusion coefficient the graph of electrodynamic model lies below that of a purely diffusive one, at the interval corresponding to discharge of the cell, and is above the latter at large values of applied voltage. This is due to the fact that the presence of a negative charge distributed inside the particle enhances insertion of lithium ions, and the positive charge enhances, correspondingly, their going out. At the same time the graph of electrodynamic model is below that of a purely diffusive one in the vicinity of zero because the concentration profile is more sloping in electrodynamic case during the switching of the regime. In the case of a variable diffusion coefficient the graph of the model with electric field, as Figures 3-5 indicate, is, in general, closer to that of chemical potential model than in the previous case, because the lithium ion - lithium ion interactions governed by the activity coefficient makes the term proportional to ∇y in divσE in the diffusion equation not so significant due to more sloping concentration profile. Comparison of Figures 3-5 shows that the relative difference between electrodynamic and non-electrodynamic models becomes more significant as the sweep rate of the applied voltage decreases. It looks like the electric field has its stable contribution to j_n^+ which is the more transparent, the less significant is hysteresis.

Figures 11, 12, 13, 14 show the profiles of dimensional concentration y vs. dimensional radial distance R at correspondingly Stage 1, Stage 2, Stage 3, Stage 4 of the cycle. Figure 11 corresponds to discharge, Figure 13 - to discharge, Figure 12 and 14 - to switching the regime.

Table II. System of model equations and boundary conditions.

Region	Value	Equation or boundary condition
$x = L_s + L_1$	C	$\epsilon_s D_{eff,s}\nabla C = i_{total}/F$
	i_2	$i_2 = i_{total}$
$L_s + L_1 > x > L_1$	C	$\epsilon_s\frac{\partial C}{\partial t} = \nabla\left(\epsilon_s D_{eff,s}\nabla C\right)$
	i_2	$i_2 = i_{total}$
	η	$\nabla\eta = \frac{i_2}{\sigma_{eff,s}} - \frac{\Re T(1-t_+^0)}{FC}\nabla C$
$x = L_1$	C	$\epsilon_s D_{eff,s}\nabla C\big\vert_{L_1+0} = \epsilon_1 D_{eff,1}\nabla C\big\vert_{L_1-0}$
$L_1 > x > 0$	y	For cylindrical particles (2.1) with (2.2)-(2.4), or (2.7) with (2.2)-(2.4). For spherical particles (3.1) with (2.2)-(2.4), or (3.2) with (2.2)-(2.4).
	C	$\epsilon_1\frac{\partial C}{\partial t} = \nabla\left(\epsilon_1 D_{eff,1}\nabla C\right) + a(1-t_+^0)j_n^+$
	i_2	$\nabla i_2 = aFj_n^+$
	η	$\nabla\eta = \frac{-i_{total}}{\sigma_{eff}} + i_2\left(\frac{1}{\sigma_{eff}} + \frac{1}{\sigma_{eff,1}}\right) - \frac{\Re T(1-t_+^0)}{FC}\nabla C$
$x = 0$	C	$\epsilon_1 D_{eff,1}\nabla C = 0$
	i_2	$i_2 = 0$

3. Spherical particles.

For spherical particles equations (2.1) and (2.7) are replaced by

$$\frac{\partial y}{\partial \tau} = \frac{1}{R^2}\frac{\partial}{\partial R}\left(R^2 f \frac{\partial y}{\partial R}\right) \tag{3.1}$$

$$\frac{\partial y}{\partial t} = \frac{1}{R^2}\frac{\partial}{\partial R}\left(R^2 \frac{D_s}{R_s^2} f \frac{\partial y}{\partial R}\right) - \frac{1}{FC_{max,s}}\mathrm{div}(\sigma E), \tag{3.2}$$

$$\mathrm{div}(E) = \frac{3}{R_s \sigma_{eff,1}} j_n^+ - \delta \frac{FC_{max,s}}{\varepsilon_0}(y_{avr} - y).$$

The corresponding set of equations from Table II has been solved numerically.

In the same way as for cylindrical particles, Figure 2 shows that in the case of a constant diffusion coefficient the electrodynamic model admits lager discharge currents during the discharge, and at higher voltages during the charge. In the case of a variable diffusion coefficient the model with electric field admits, in general, lager amplitudes of current in hysteresis, as Figures 6-8 indicate. In this case the graphs of electrodynamic model lie closer to non-electrodynamic ones than in the previous. The relative difference between electrodynamic and non-electrodynamic models is more significant as the sweep rate of the applied voltage becomes smaller.

Comparing cyclic voltammograms for spherical (Figures 6-8) and for cylindrical particles (Figures 3-5) one may see that the influence of electrostatic field is more significant in the case of cylindrical particles because in that case the charge that produces this field occupies larger part of a space.

4. Conclusions.

We have made a simulation of the cycling of lithium cell with microporous carbon electrode under potentiodynamic control. We have compared the predictions of the models in which electric field is not considered (CPM, DFM) and the ones in which electrostatic interaction of lithium ions between each other and with the distribution of charge in the bulk of carbon electrode is taken into account (CPME, DFME). We have observed that there is a considerable difference between the results predicted by both models. The form of the particles does not have a significant influence on the predictions of both models. In the case of a constant diffusion coefficient the electrodynamic model allows for

lager discharge currents. In the case of a variable diffusion coefficient the model with electric field allows for lager sweep of current in general. The models without electric field predict steeper profiles of concentration of lithium ions inside the particle. The results indicate that the electrostatic interactions does matter, that the kinetic parameters obtained with the purely diffusive (DFM) or chemical potential model (CPM) may not represent the real kinetics of the system, and that the cell should be modelled using electrodynamic approach to get more adequate results.

References

1. G. G. Botte and R. E. White, J. Electrochem. Soc. **148** ((1) 2001), A54–A66.
2. G. G. Botte, B. A. Johnson, and R. E. White, J. Electrochem. Soc. **146** (1999), 914.
3. I. O. Polyakov, V. K. Dugaev, Z. D. Kovalyuk, and V. I. Litvinov, Russian Journal of Electrochemistry **Vol. 33, No. 1** (1997), 21Ц25.
4. R. Kanno, Y. Kawamoto, Y. Takeda, S. Ohashi, N. Imanishi, and O. Yamamoto, J. Electrochem. Soc. **139** (1992), 3397.
5. S.-I. Lee, Y.-S. Kim, H.-S. Chun, Electrochim. Acta **47** (2002), 1055–1067.
6. M. W. Verbrugge and B. J. Koch, J. Electrochem. Soc. **143** (1996), 600.

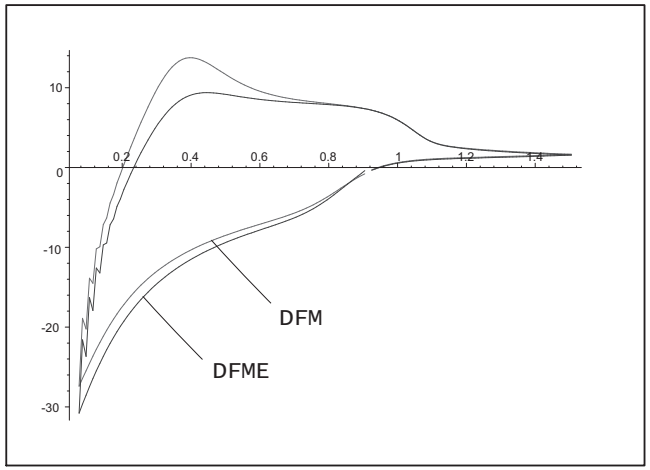

Figure 1. Current density (A/m^2) vs. applied voltage (V) at scan rate 10mV/s for cylindrical particles for purely diffusive model with (DFME) and without electric field (DFM).

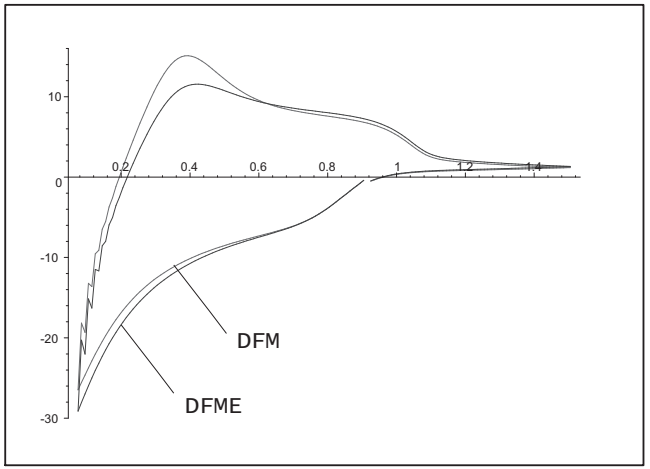

Figure 2. Current density (A/m^2) vs. applied voltage (V) at scan rate 10mV/s for spherical particles for purely diffusive model with (DFME) and without electric field (DFM).

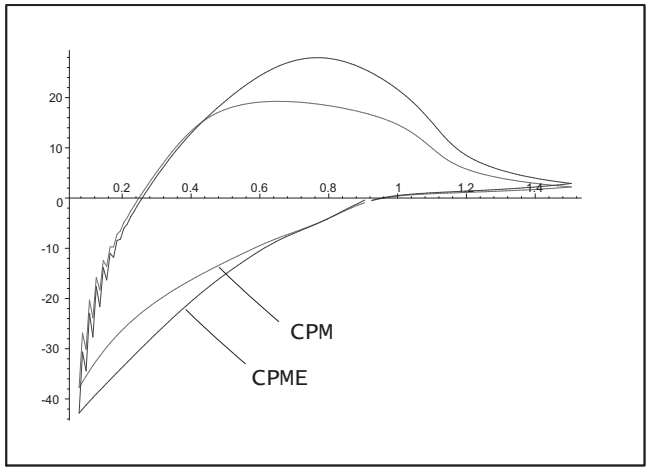

Figure 3. Current density (A/m^2) vs. applied voltage (V) at scan rate 10mV/s for cylindrical particles for chemical potential model with (CPME) and without electric field (CPM).

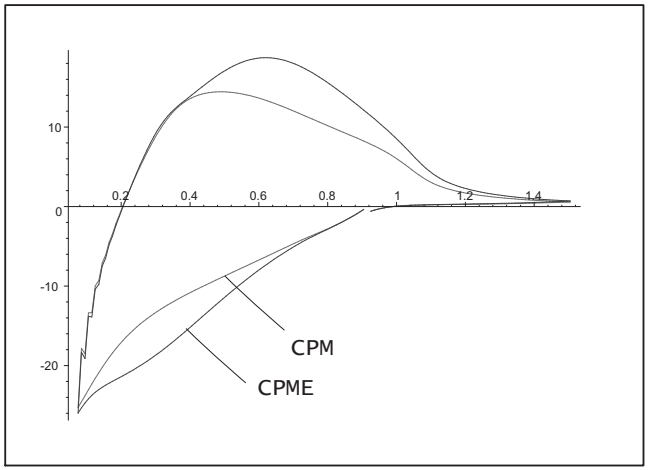

Figure 4. Current density (A/m^2) vs. applied voltage (V) at scan rate 5mV/s for cylindrical particles for chemical potential model with (CPME) and without electric field (CPM).

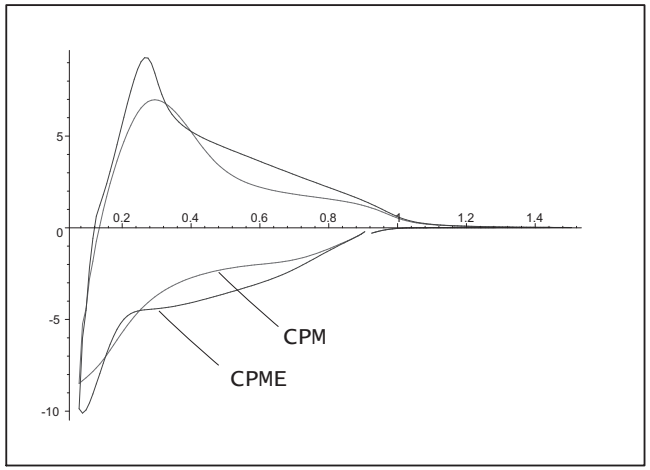

Figure 5. Current density (A/m^2) vs. applied voltage (V) at scan rate 1mV/s for cylindrical particles for chemical potential model with (CPME) and without electric field (CPM).

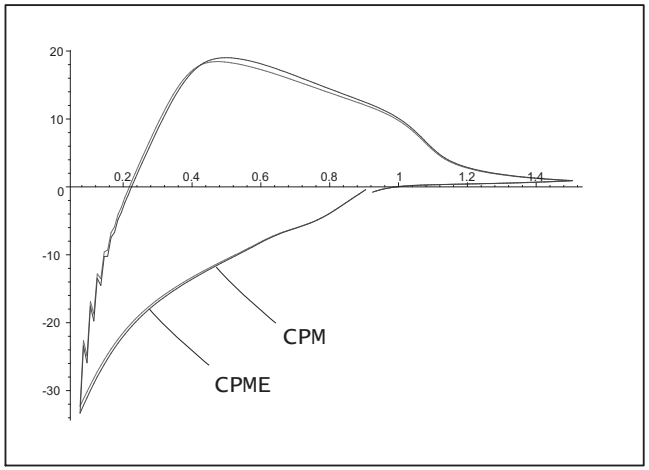

Figure 6. Current density (A/m^2) vs. applied voltage (V) at scan rate 10mV/s for spherical particles for chemical potential model with (CPME) and without electric field (CPM).

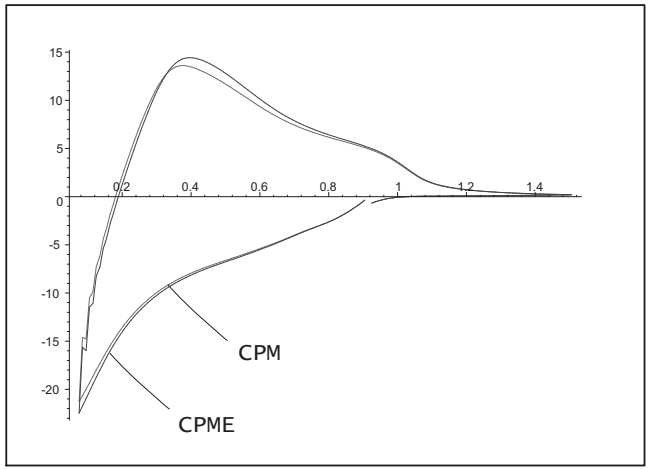

Figure 7. Current density (A/m^2) vs. applied voltage (V) at scan rate 5mV/s for spherical particles for chemical potential model with (CPME) and without electric field (CPM).

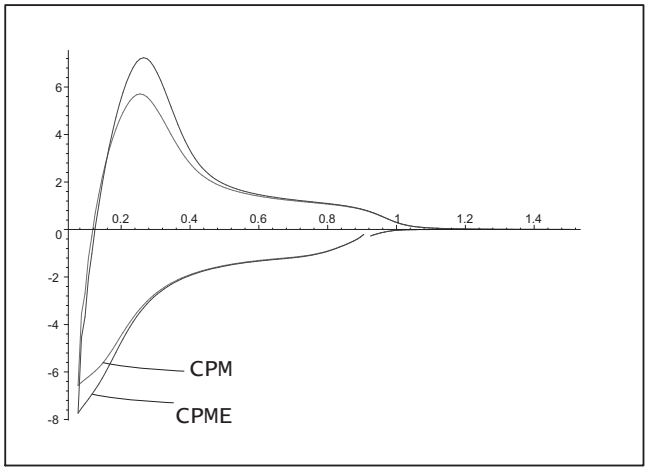

Figure 8. Current density (A/m^2) vs. applied voltage (V) at scan rate 1mV/s for spherical particles for chemical potential model with (CPME) and without electric field (CPM).

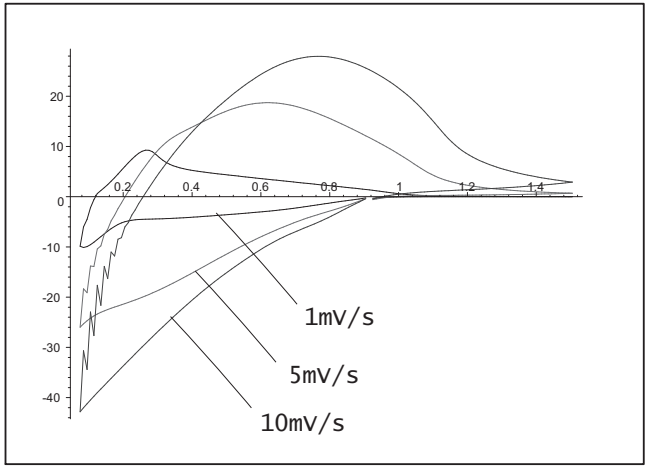

Figure 9. Comparison of current density (A/m^2) vs. applied voltage (V) at scan rates 10mV/s, 5mV/s and 1mV/s for cylindrical particles for chemical potential model with electric field .

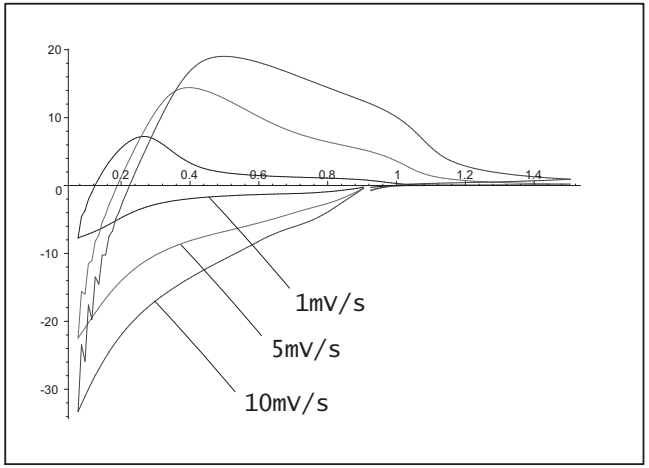

Figure 10. Comparison of current density (A/m^2) vs. applied voltage (V) at scan rates 10mV/s, 5mV/s and 1mV/s for spherical particles for chemical potential model with electric field .

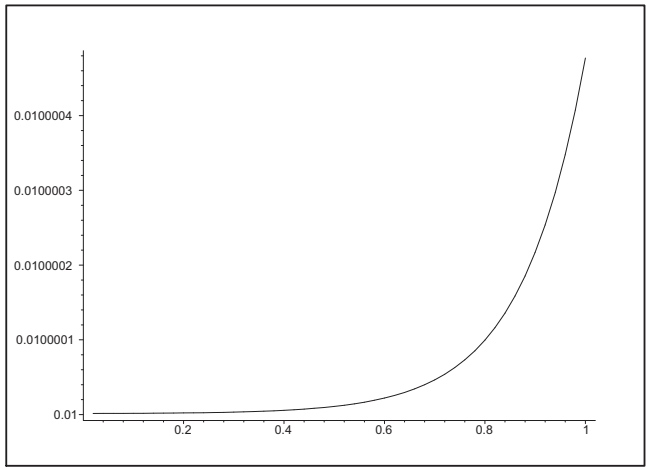

Figure 11. Profile of dimensionless concentration vs. dimensionless radial distance for cylindrical particles located at distance $L_1/2$ from current collector, for chemical potential model with electric field at applied voltage Uapp=0,91489V.

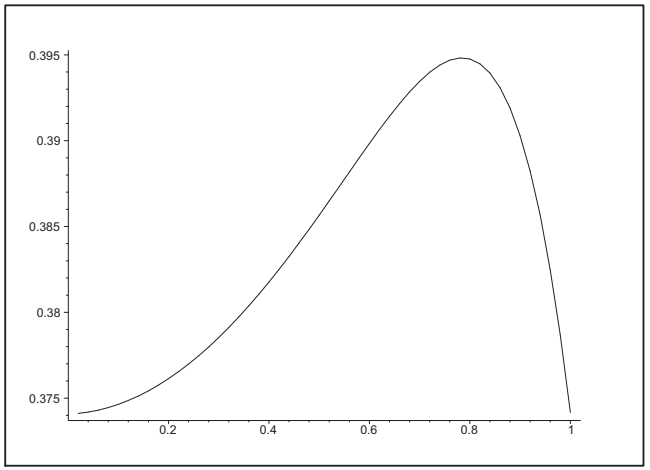

Figure 12. Profile of dimensionless concentration vs. dimensionless radial distance for cylindrical particles located at distance $L_1/2$ from current collector, for chemical potential model with electric field at applied voltage Uapp=0,31489V.

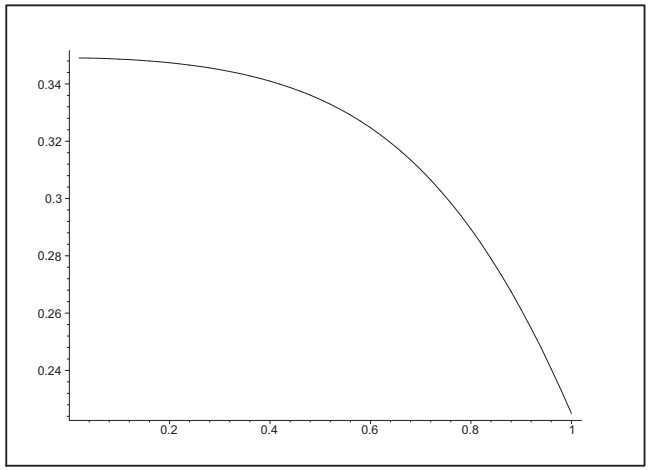

Figure 13. Profile of dimensionless concentration vs. dimensionless radial distance for cylindrical particles located at distance $L_1/2$ from current collector, for chemical potential model with electric field at applied voltage Uapp=0,51489V.

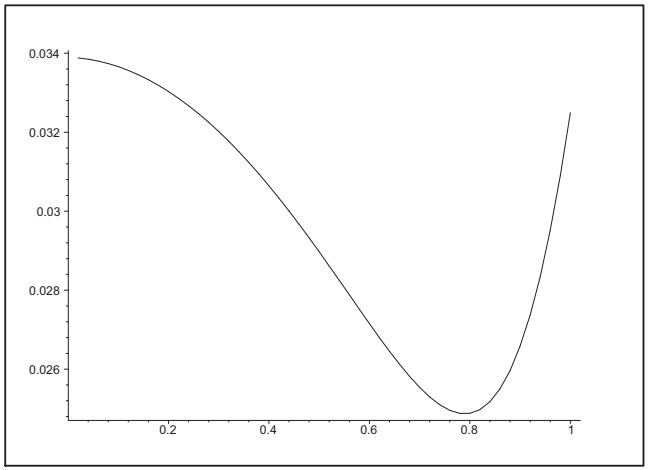

Figure 14. Profile of dimensionless concentration vs. dimensionless radial distance for cylindrical particles located at distance $L_1/2$ from current collector, for chemical potential model with electric field at applied voltage Uapp=0,81489V.

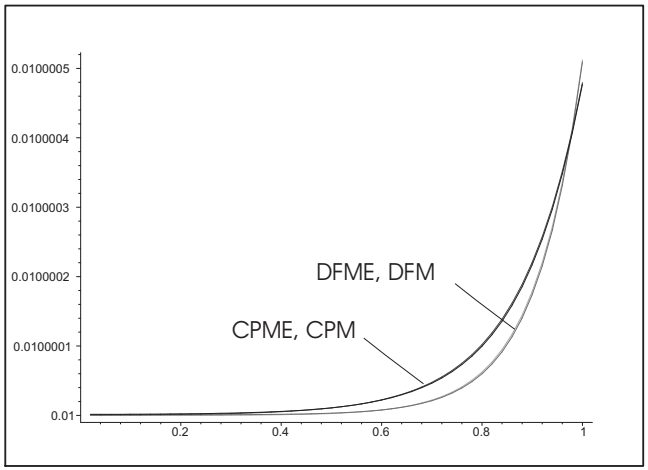

Figure 15. Comparison of profiles of dimensionless concentration vs. dimensionless radial distance for cylindrical particles located at distance $L_1/2$ from current collector, for purely diffusive model with and without electric field and for chemical potential model with and without electric field at applied voltage Uapp=0,91489V.

CONDENSED MATTER PHYSICS

The journal **Condensed Matter Physics** is founded in 1993 and published by Institute for Condensed Matter Physics of the National Academy of Sciences of Ukraine.

AIMS AND SCOPE: The journal **Condensed Matter Physics** contains research and review articles in the field of statistical mechanics and condensed matter theory. The main attention is paid to physics of solid, liquid and amorphous systems, phase equilibria and phase transitions, thermal, structural, electric, magnetic and optical properties of condensed matter. Condensed Matter Physics is published quarterly.

ABSTRACTED/INDEXED IN:

- Chemical Abstract Service, Current Contents/Physical, Chemical&Earth Sciences
- ISI Science Citation Index-Expanded, ISI Alrting Services
- INSPEC
- Elsevier Bibliographic Databases (EMBASE, EMNursing, Compendex, GEOBASE, Scopus)
- "Referativnyi Zhurnal"
- "Dzherelo"

CONTACT INFORMATION:
Institute for Condensed Matter Physics
of the National Academy of Sciences of Ukraine
1 Svientsitskii Str., 79011 Lviv, Ukraine
Tel: +380(322)760908; Fax: +380(322)761158
E-mail: cmp@icmp.lviv.ua http://www.icmp.lviv.ua